Coordinated Operation of Multi-Neighborhood Energy Systems: A Bi-Level Optimization Approach

Carla Wüller[a], Simon Stamen[a], Rita Streblow[a], Dirk Müller[a]

[a] *RWTH Aachen University, E.ON Energy Research Center, Institute for Energy Efficient Buildings and Indoor Climate, Aachen, Germany, carla.wueller@eonerc.rwth-aachen.de, CA*

Abstract:

The increasing integration of distributed renewable energy resources in residential neighborhoods has the potential to create opportunities for local energy sharing. However, this integration also introduces coordination challenges among autonomous actors. The present paper proposes a bi-level optimization framework for coordinating a multi-neighborhood energy system that encounters electricity as well as heat demands. The proposed framework employs a leader-follower structure, wherein a system operator coordinates energy flows between neighborhoods and to the higher-level grid, minimizing the transaction costs from internal coordination and external grid exchange of the multi-neighborhood energy system, while individual neighborhoods optimize their respective costs. The optimization model employs the Karush-Kuhn-Tucker reformulation and a strong duality substitution. The bi-level optimization model is benchmarked against two approaches: an individual approach and a centrally coordinated approach. The model is solved for three archetypical German neighborhoods across representative winter, transition, and summer periods.

The findings indicate that bi-level optimization accomplishes an increase of shared energy among the neighborhoods nearly by a factor of three, resulting in a reduction of approximately 11 MWh in electricity imports for the multi-neighborhood energy system over the course of a week during winter. The system-wide cost reduction is equivalent to a centralized control approach, with a cost reduction of up to 65 % compared to the individual approach, while maintaining individual neighborhood objectives. In contradistinction to centralized approaches, which carry the risk of placing individual neighborhoods at a disadvantage, the bi-level framework ensures that no neighborhood will incur costs that exceed those associated with standalone operation.

Keywords:

Bi-level optimization, KKT reformulation, Energy Sharing, Multi-energy systems, Interconnected Neighborhoods.

1. Introduction

The energy transition has fundamentally altered power system operation. The decline in costs associated with photovoltaic systems and battery storage has accelerated adoption of distributed generation. Individual users have transitioned from passive consumption to active participation by feeding energy into the grid at decentralized levels. This emergence of prosumers—users who flexibly produce and consume energy [1]—fundamentally alters system operation. Historically, electric power flowed uni-directionally from central generating units through transmission and distribution networks to end users [2]. Decentralized generation has transformed this into bi-directional flow, creating substantial coordination challenges and necessitating novel control methodologies. Recent regulatory developments have formalized mechanisms for local energy sharing. The EU Clean Energy Package [3] established legal frameworks enabling end users to share energy through public grids, with national implementations like the German draft law on collective self-consumption [4] providing specific provisions for non-commercial residential applications. These regulations aim to reduce electricity imports through local balancing and decentralized utilization, lowering costs for prosumers [5] while reducing transmission losses and improving renewable integration [6].

In residential contexts, energy systems manifest as neighborhood energy systems wherein multiple buildings share local generation, storage, and loads [7]. The structural homogeneity that characterizes most neighborhoods often leads to similar demand and generation profiles. The paper's underlying assumption is that the integration of multiple neighborhoods into a multi-neighborhood energy system (MNES) represents a promising approach to leveraging the local potential of energy sharing. While individual neighborhoods optimize their own objectives, system-level benefits emerge from coordinated operation: shared flexibility resources,

mutual backup during supply-demand mismatches, and collective market participation. However, realizing these benefits requires coordination mechanisms that respect neighborhood autonomy. These mechanisms must guarantee that participation never leaves an individual neighborhood worse off than standalone operation while enabling efficient collective operation—a challenge compounded by the presence of multiple agents with potentially conflicting objectives [1]. Multi-energy systems coupling electricity and heat through heat pumps, combined heat and power (CHP) plants, and thermal storage add operational flexibility but further complicate coordination. [8, 9]

This work investigates bi-level optimization as a game-theoretical approach to model a residential MNES, addressing the question: How can multiple autonomous multi-energy neighborhoods coordinate their operation to minimize collective costs while preserving individual decision-making authority, and how does this coordination perform under varying seasonal conditions and a dynamic market price?

This paper is organized as follows: Section 2 reviews the state of the art in bi-level optimization for energy systems and identifies research gaps. Section 3 presents the mathematical models and the case study setup. Section 4 evaluates the coordination performance and analyzes the seasonal cost impacts on the energy system and its neighborhoods. Finally, Section 5 concludes the paper and outlines future research.

2. Literature Review

This section reviews existing applications of bi-level optimization in energy systems, with a focus on hierarchical coordination frameworks for interconnected microgrids and neighborhood systems. It analyzes prior work to identify specific research gaps that motivate the present study.

2.1. Interconnected Neighborhoods

Neighborhoods represent geographically proximate clusters of buildings that share local generation, storage, and loads through interconnected infrastructure [10]. Each neighborhood typically contains distributed energy resources such as photovoltaic systems, battery storage, and sector-coupling technologies like heat pumps or CHP units. When multiple such neighborhoods interconnect through the medium voltage grid, a MNES emerges that enables energy exchange among autonomous entities while each maintains individual grid connection and decision-making authority. This structure aligns with the concept of multi-microgrid systems, where individual microgrids can operate autonomously but benefit from mutual support through controllable interconnections [11]. While energy sharing concepts range from peer-to-peer trading to collective self-consumption [12], this work considers a hierarchical structure for MNES. In this model, autonomous neighborhoods exchange energy via a coordinating entity. This structure bridges the gap between two extremes: fully centralized systems, which achieve global optimality but disregard neighborhood autonomy and privacy, and fully decentralized approaches, which preserve autonomy but suffer from cooperation deficiencies [10, 13].

2.2. Bi-level Optimization for Multi-Neighborhood Coordination

The hierarchical structure inherent in multi-neighborhood coordination naturally maps to the leader-follower framework of Stackelberg games. Game theory provides mathematical tools for modeling interactions between multiple decision-makers with potentially conflicting objectives, ensuring individual rationality [14]. Non-cooperative games, particularly Stackelberg formulations, align with the autonomous decision-making characteristic of residential energy systems where each neighborhood optimizes its own objective while responding to coordination mechanisms [6, 13]. Bi-level optimization provides the mathematical framework for implementing Stackelberg games through nested optimization problems. The upper-level leader determines coordination mechanisms, typically internal pricing schemes, anticipating how lower-level followers will respond. Each follower optimizes autonomously based on local constraints and the leader's decisions, with only the follower's optimal response being feasible for the leader [15]. The coordinator lacks direct control over neighborhood assets and must design incentive mechanisms that guide autonomous agents toward collectively beneficial outcomes. In the MNES context, the coordinating entity acts as the upper-level leader, setting internal energy exchange prices, while each neighborhood operates as a lower-level follower that optimizes its own energy management based on these prices and local objectives.

2.3. Review of Bi-level Applications in Energy Systems

In energy systems, bi-level frameworks capture Stackelberg-type interactions between different actors such as market operators and participants, grid operators and microgrids, or coordinating entities and autonomous subsystems [6]. Two fundamental problem classes exist: cooperative formulations where agents contribute to a common system objective, and non-cooperative formulations where each agent optimizes its own objective function. Cooperative approaches include Zhang et al. [16], who developed a model for unit commitment in interconnected microgrids using KKT reformulation with robust optimization, and Ahmadi et al. [17], who addressed multi-energy neighborhood cooperation through iterative progressive hedging. However, cooperative frameworks assume aligned incentives and shared objectives, which may not reflect the autonomous decision-making prevalent in decentralized residential systems.

Non-cooperative Stackelberg formulations dominate the literature on electricity markets and microgrid coordination. Applications span market bidding [18], multi-energy pricing between retailers and consumers [19], and supplier-consumer welfare optimization [20]. Lu et al. [21] modeled a grid operator optimizing security and losses (upper level) with cost-minimizing microgrids (lower level), solved via NSGA-II. Karimi et al. [22] formulated a distribution network operator with multiple objectives coordinating multiple cost-minimizing microgrids through KKT reformulation. Jani et al. [23] developed a two-stage day-ahead and real-time framework where a microgrid community (upper level) coordinates individual microgrid dispatch (lower level). Zhuang et al. [24], Boloukat et al. [25], and Fu et al. [26] proposed similar single leader-multiple follower structures with KKT reformulation. Matamala et al. [27] developed a multiple leader-single follower model for power-to-X expansion planning.

Solution methodologies divide into heuristic and exact approaches. Heuristic methods—Particle Swarm Optimization [18, 19], NSGA-II [21, 28], Reinforcement Learning [20]—handle nonlinearities but lack optimality guarantees. Exact KKT reformulation, applicable when the lower level is a linear program, transforms the bi-level problem into a single-level MILP by replacing the lower level with its optimality conditions: primal feasibility, dual feasibility, stationarity, and complementarity constraints [15, 29]. The prevalence of KKT approaches in neighborhood-scale applications [22–24, 27] demonstrates their suitability for such systems.

Temporal scopes vary considerably across the literature. Boloukat et al. [25] and Lin et al. [28] do not consider explicit operational optimization. Most studies with operational optimization evaluate single-day horizons with 24 h resolution [16, 19, 22, 23]. Only Matamala et al. [27] considers annual operational optimization (8760 h), though focused on industrial power-to-X rather than residential systems. Some works incorporate stochastic or robust methods for renewable generation uncertainty [16, 23, 27]. Multi-energy system coupling receives limited attention, with only Ahmadi et al. [17], Hong et al. [19], and Matamala et al. [27] incorporating heat sectors. However, none systematically evaluate how sector coupling influences bi-level coordination in residential multi-neighborhood contexts across varying seasonal conditions. Table 1 summarizes the reviewed studies, differentiating by game type, agent structure, solution method, multi-energy consideration, and optimization horizon.

Table 1. *Representative bi-level optimization studies in energy systems.*

Reference	Game Type	Upper Level	Lower Level	Method	Multi-Energy	Horizon
Zhang et al. [16]	Cooperative	Multiple	Multiple	KKT	No	1 day
Ahmadi et al. [17]	Cooperative	Single	Multiple	Iterative	Yes	1 day
Lin et al. [28]	Both	Multiple	Multiple	NSGA	No	–
Zhang et al. [18]	Non-coop.	Multiple	Single	PSO	No	1 day
Hong et al. [19]	Non-coop.	Single	Multiple	PSO	Yes	1 day
Wang et al. [20]	Non-coop.	Multiple	Multiple	RL	No	1 day
Lu et al. [21]	Non-coop.	Single	Multiple	NSGA	No	1 day
Matamala et al. [27]	Non-coop.	Multiple	Single	KKT	Yes	365 days
Karimi et al. [22]	Non-coop.	Single	Multiple	KKT	No	1 day
Jani et al. [23]	Non-coop.	Single	Multiple	KKT	No	1 day
Zhuang et al. [24]	Non-coop.	Single	Multiple	KKT	No	1 day
Boloukat et al. [25]	Non-coop.	Single	Multiple	KKT	No	–
Fu et al. [26]	Non-coop.	Single	Multiple	KKT	No	1 day
This work	Non-coop.	Single	Multiple	KKT	Yes	3 seasons $\times$ 7 days

Despite extensive literature on bi-level optimization in energy systems, three specific gaps motivate this work. First, existing studies primarily address industrial microgrids or market-oriented applications. The explicit modeling of residential neighborhood energy sharing that guarantees no individual neighborhood is disadvantaged by its participation while enabling coordinated operation remains under-explored. Second, few bi-level studies integrate electricity-heat coupling in residential contexts. The coordination potential of distributed heat pumps, CHP units, and thermal storage across multiple autonomous neighborhoods has not been systematically investigated. Third, the dominance of single-day evaluations obscures how coordination mechanisms perform under varying seasonal conditions. Residential energy systems exhibit strong seasonal variations in heat demand and renewable generation, yet whether bi-level coordination strategies remain effective across winter, summer, and transition periods is unclear. This paper addresses these gaps through a KKT-based non-cooperative bilevel framework for residential multi-energy neighborhoods, evaluated across three representative seasonal weeks.

3. Methodology

This section presents the methodological framework for coordinating multiple autonomous neighborhoods. First, the MNES structure and optimization framework are introduced. Subsequently, three optimization models with distinct pricing structures are described. The bi-level model is then formulated mathematically and reformulated using KKT conditions. Finally, the case study design is presented.

3.1. Multi-Neighborhood Energy System and Optimization Framework

The MNES consists of multiple interconnected neighborhood energy systems, each serving residential prosumers with coupled electricity and heat supply. The optimization framework employs a mixed-integer linear program (MILP) following a four-level hierarchy: device level, building level, neighborhood level, and MNES level. This structure enables bottom-up energy balance aggregation while maintaining flexibility for different coordination mechanisms.

The physically-based model establishes component-specific constraints and energy balance equations at all levels, enforcing demand satisfaction and technical capacity limits. Each neighborhood integrates electric and thermal connections internally, while inter-neighborhood interactions are limited to electrical connections. The hierarchical structure is formalized as devices $d \in D$ assigned to buildings $b \in B$, buildings to neighborhoods $n \in N$, and all neighborhoods to one MNES. The rolling horizon approach is employed, thereby ensuring that operational optimization is conducted exclusively for a designated period of time T.

3.2. Optimization Models and Pricing Structures

Three optimization models are investigated: decentralized, centralized and bi-level. Figure 1 visualizes the structural differences and pricing mechanisms.

Decentral model: Each neighborhood n independently minimizes its costs without inter-neighborhood coordination or energy sharing, representing current practice. The objective minimizes the total costs for the neighborhood. These consist of the difference between the import costs (buying price p_t^{b} plus grid fees p^{fees}), the operational costs ($C_{t,n}$) and export revenue (selling price p^{s}):

$$\min_{y_n} \quad \sum_{t \in T} (C_{t,n} - p^{\mathsf{s}} P_{t,n}^{\mathsf{Exp}} + \left(p_t^{\mathsf{b}} + p^{\mathsf{fees}}\right) P_{t,n}^{\mathsf{Imp}}), \tag{1}$$

subject to device and balance constraints (Appendix A). Decision variables y_n encompass device operation, storage states, and grid exchanges $P_{t,n}^{\mathsf{Imp}}$ and $P_{t,n}^{\mathsf{Exp}}$. Grid fees apply at neighborhood level.

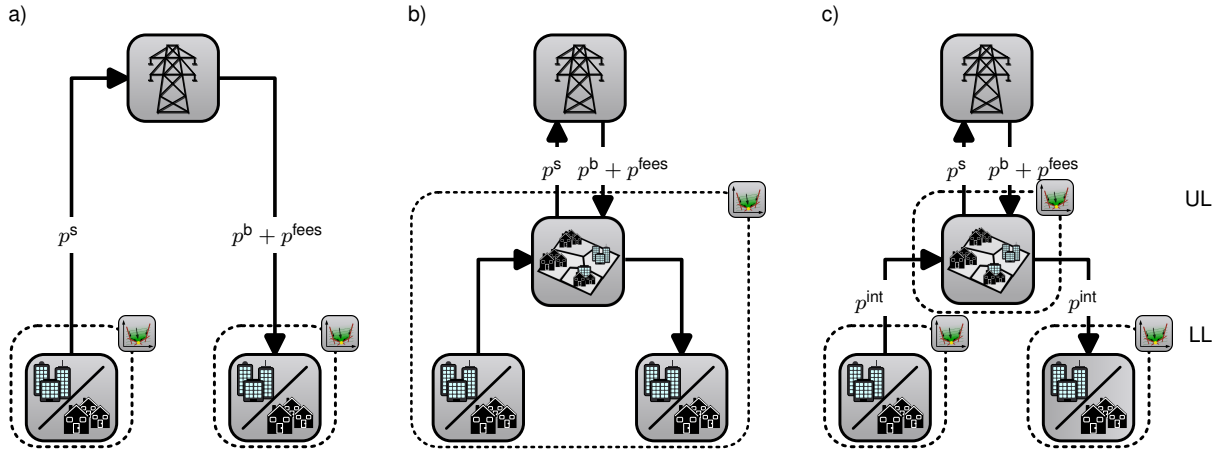

Figure 1. *Price structure for decentralized (a), centralized (b), and bi-level (c) models. Black arrows denote power flows with allocated costs. Dashed lines indicate optimization boundaries.*

Central model: The optimization of the MNES is achieved through the actions of a single agent. Total system costs are minimized, with aggregated imports P_t^{Imp} and exports P_t^{Exp} of the MNES to the higher-level grid and the operational costs of every neighborhood ($C_{t,n}$):

$$\min_{P_t^{\mathsf{Exp}}, P_t^{\mathsf{Imp}}, y} \quad \sum_{t \in T} (\sum_{n \in N} C_{t,n} - p^{\mathsf{s}} P_t^{\mathsf{Exp}} + \left(p_t^{\mathsf{b}} + p^{\mathsf{fees}}\right) P_t^{\mathsf{Imp}}). \tag{2}$$

Grid fees apply at MNES level, exempting internal exchanges. Internal energy sharing between neighborhoods uses the average of selling and buying prices (p_t^{es}), distributing cost advantages equally. Allocation factors weight neighborhood costs between internal and external prices: the export ratio (ϕ_t^E) determines the share of total generation P_t^{Gen} exported externally, while the generation ratio (ϕ_t^I) quantifies the share of total system supply covered by internal generation versus external imports:

$$p_t^{\mathsf{es}} = \frac{p^{\mathsf{s}} + p_t^{\mathsf{b}}}{2}, \quad \phi_t^E = \frac{P_t^{\mathsf{Exp}}}{P_t^{\mathsf{Gen}}}, \quad \phi_t^I = \frac{P_t^{\mathsf{Gen}}}{P_t^{\mathsf{Gen}} + P_t^{\mathsf{Imp}}}.$$

$$p_t^{\mathsf{b,int}} = \phi_t^I p_t^{\mathsf{es}} + \left(1 - \phi_t^I\right) \left(p_t^{\mathsf{b}} + p^{\mathsf{fees}}\right) \tag{3}$$

$$p_t^{\mathsf{s,int}} = \left(1 - \phi_t^E\right) p_t^{\mathsf{es}} + \phi_t^E p_t^{\mathsf{s}} \tag{4}$$

$$C_{t,n} = P_{t,n}^{\mathsf{Imp}} \cdot p_t^{\mathsf{b,int}} - P_{t,n}^{\mathsf{Exp}} \cdot p_t^{\mathsf{s,int}} \tag{5}$$

Bi-level model: This model follows Stackelberg structure with the MNES operator as leader coordinating multiple neighborhoods (followers) via internal coordination price p_t^{int}, bounded by external prices to prevent arbitrage. The upper-level (UL) MNES operator minimizes transaction costs from internal coordination and external grid exchange:

$$\min_{x,y} \quad \sum_{t \in T} \left(\sum_{n \in N} p_t^{\mathsf{int}} P_{t,n} - p^{\mathsf{s}} P_t^{\mathsf{Exp}} + \left(p_t^{\mathsf{b}} + p^{\mathsf{fees}}\right) P_t^{\mathsf{Imp}} \right), \tag{6}$$

subject to MNES power balance

$$\sum_{n \in N} P_{t,n} = P_t^{\mathsf{Exp}} - P_t^{\mathsf{Imp}}, \quad \forall t \in T, \tag{7}$$

and price bounds

$$p^{\mathsf{s}} \leq p_t^{\mathsf{int}} \leq p_t^{\mathsf{b}} + p^{\mathsf{fees}}, \quad \forall t \in T. \tag{8}$$

UL variables $x = \{p_t^{\mathsf{int}}, P_t^{\mathsf{Exp}}, P_t^{\mathsf{Imp}}\}$ include internal price and MNES grid exchange.
Each lower-level (LL) neighborhood n minimizes individual costs:

$$\min_{y_n} \quad \sum_{t \in T} \left(C_{t,n} - p_t^{\mathsf{int}} P_{t,n}\right), \tag{9}$$

subject to device constraints and balances. $C_{t,n}$ denotes operational costs, $P_{t,n}$ net electricity exchange (positive for export from the neighborhood). Variables y_n include device operation, storage states, and heat flows. Device constraints cover photovoltaic generation, wind power, heat pumps, CHP units, electric heaters, battery storage, and thermal storage. Heat and electricity balances ensure demand satisfaction through appropriate combinations of generation, storage operation, and grid exchange. Inter-neighborhood power exchange is modeled without network losses.

The bi-level problem is reformulated using Karush-Kuhn-Tucker (KKT) conditions [23, 24]. Binary variables preventing simultaneous battery charging/discharging are replaced by degradation cost terms, rendering the lower-level programs fully linear and thus amenable to KKT reformulation [29]. The KKT conditions comprise primal feasibility, dual feasibility — with $\pi_{t,n}^i \geq 0$ for inequality constraints and unrestricted $\lambda_{t,n}^j$ for equality constraints — stationarity ($\nabla_{y_n} \mathcal{L}_{t,n} = 0$), and complementarity ($\pi_{t,n}^i \mathcal{C}_{t,n}^{i,\mathsf{ineq}} = 0$). The complementarity conditions are linearized via the big-M method, introducing one binary variable per inequality constraint per neighborhood and time step. Strong duality then replaces the bilinear term $p_t^{\mathsf{int}} P_{t,n}$ in the upper-level objective with the lower-level dual objective [22], yielding a single-level MILP. The KKT reformulation assumes the system operator has complete knowledge of neighborhood models, which serves as a tractable mathematical abstraction.

3.3. Case Study Design

Full-year hourly optimization is computationally prohibitive for multi-neighborhood systems. Time series for electricity/heat demand, PV/wind generation, and day-ahead prices are aggregated into three representative weeks (winter, transition, summer) using hierarchical clustering [30] with hourly resolution. Demand and generation profiles use 2015 weather data from the German weather service [31]; electricity and gas prices are sourced from 2023-2024 SMARD data [32].

The framework is evaluated using three archetypical German neighborhoods from [33] located in Aachen: rural (Type 1), suburban (Type 2), and urban (Type 6). Building counts, types, ages, and floor areas follow [33] specifications. All buildings are assumed retrofitted. Demand profiles of the buildings are generated using the Districtgenerator tool [34]. Each neighborhood features a central energy hub supplying heat via district heating (50 °C supply, 40 °C return, lossless). Each building is equipped with its own drinking hot water supply, which is

not managed or accounted for by the energy hub. Consequently, this aspect is not included in the overall assessment. Figure 2 shows the system architecture. The rural neighborhood consists of detached houses with low building density and employs heat pumps, electric heaters, and thermal storage for heating; PV, one wind power plant, and battery storage provide electricity. The suburban neighborhood with moderate density at the urban fringe uses similar technologies but excludes wind due to space constraints. The urban neighborhood is characterized by dense inner-city multi-family houses forming street blocks and faces severe space limitations: a CHP plant provides heat and power, supplemented by electric heaters and thermal storage; renewable power generation is only possible when biogas is used. This heterogeneous design enables evaluation of coordination mechanisms when neighborhoods have fundamentally different supply-demand characteristics. The design of the heat generation systems and thermal storage was carried out by EHDO [35], with PV and battery sizes following values from [33]. Table 2 summarizes key characteristics.

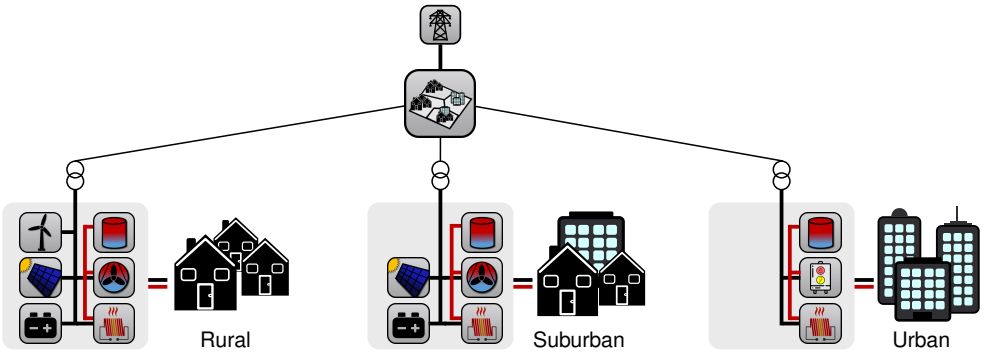

Figure 2. *Case study system architecture with three archetypical neighborhoods.*

Operational costs for PV, wind, and battery follow [23]. Battery degradation costs are calculated from investment costs C^{Inv}, capacity E^{Bat}, and life cycle numbers LCN as $c^{\text{Bat}} = \frac{C^{\text{Inv}}}{E^{\text{Bat}} \cdot LCN}$. Heat pump and CHP costs are derived from fixed operational costs [36], converted to power-specific values assuming typical full load hours. For CHP, the costs for the gas used are also taken into account. Thermal storage costs are converted from annual operational costs to power-specific values. All other technical parameters and cost values are taken from the municipal heat planning technology catalog [36], which provides standardized reference data for renewable heating technologies in the German context. Rolling horizon optimization is performed with a 48-hour prediction and a 24-hour control horizon, chosen to align with day-ahead price forecasts.

Table 2. *Key characteristics of investigated neighborhoods.*

	Rural	Suburban	Urban
Annual electricity demand (MWh)	434	1472	357
Annual heat demand (MWh_{th})	1491	4019	941
Buildings (single / multi family)	28 / 14	88 / 43	0 / 32
Heat pumps (kW_{th})	410	1200	–
Electric heaters (kW_{th})	220	700	230
CHP units (kW_{th})	–	–	150
Thermal storage (m^3)	180	520	50
PV capacity (kW_p)	120	1350	–
Wind capacity (kW_p)	2750	–	–
Battery capacity (kWh)	120	1350	–

4. Results and Discussion

This section analyzes the bi-level optimization results, beginning with the internal price mechanism's effect on system coordination during a transition week. We then evaluate the model's seasonal performance. All results are benchmarked against central and decentral optimization models.

4.1. System Coordination for Bi-level Optimization

Figure 3 depicts power flows, prices, and device operation for the bi-level optimization during the transition week. The MNES power flow represents the residual of neighborhood exchanges and varies between $-1.9\,\text{MW}$ peak import during night hours and $1.2\,\text{MW}$ peak export during midday. The three neighborhoods frequently balance each other MNES-internally. The rural neighborhood exports most frequently due to high renewable generation relative to demand. The suburban neighborhood, which has the largest total demand, dominates the magnitude of MNES power flow and contributes the most to import peaks (e.g., March 4). The urban neighborhood typically operates counter-cyclically to the overall MNES balance: when the MNES requires

grid import, urban exports from CHP generation. This complementary behavior enhances MNES-level self-sufficiency.

The internal price fluctuates between the feed-in price (lower bound, $7.34\ \mathrm{ct/kWh}$) and the buy price plus grid fees (dynamic upper bound). The price reaches its upper bound during MNES import periods (e.g., midday March 4, night March 7) and its lower bound during export periods (e.g., midday March 2). This price signal coordinates neighborhood behavior: battery discharge and CHP generation occur during high-price periods, reducing necessary grid import. Peak internal prices reach approximately $23\,\mathrm{ct/kWh}$ when both batteries and CHP operate simultaneously, reflecting the marginal cost of avoiding grid import. This strategic price increase by the upper-level operator incentivizes neighborhoods to utilize flexible devices, aligning demand and generation. When import becomes unavoidable and no additional internal energy is available, the internal price equals the buy price (e.g., March 2, 22:00). Conversely, on March 4 midday, a demand peak occurs in the suburban neighborhood when external spot prices remain below CHP generation costs, demonstrating responsiveness to the external buy price.

The suburban and urban neighborhoods employ fundamentally different heat provision strategies due to their technology portfolios. In the suburban neighborhood, the heat pump charges thermal storage during midday when PV generation is high and internal prices are low (March 1, 2, 5). The storage system is then discharged during morning demand peaks, when prices are elevated. On March 4, full-load operation occurs despite high internal prices, anticipating even higher subsequent spot prices. End-of-horizon effects are visible on the last day when storage is fully discharged.

The urban neighborhood CHP operates inversely: heat production is minimal during low internal prices (March 1, 2, 5, 7) as the electric heater becomes more economical. During high internal prices, the CHP runs at full load for simultaneous electricity generation and thermal storage charging. From evening March 3 through midday March 4, the CHP operates continuously until external prices, and consequently the internal price, fall below its operational costs. On the afternoon of March 3, a concurrent occurrence of CHP and battery discharge, in conjunction with suburban thermal storage discharge, signifies an acute electricity demand, necessitating the full utilization of MNES flexibility. On March 7, the suburban and rural neighborhoods export excess electricity when other neighborhoods have no demand and thermal storage is saturated. The urban neighborhood imports simultaneously to supply heat via electric heater, demonstrating intra-MNES load balancing.

These results demonstrate that the internal price effectively coordinates MNES-beneficial device operation. Thermal flexibility is actively utilized, and both the price level and its bounds influence operational decisions. CHP-based heat provision differs fundamentally from heat pump operation: heat is produced and stored when electricity generation can be beneficially utilized within the MNES rather than purely following heat demand.

4.2. Effects of the Optimization Models

This section compares the optimization approaches regarding their impact on neighborhood and MNES-level costs as well as operational strategies. Figure 4 illustrates the internal price dynamics for central and bi-level optimization models during the summer week, alongside the residual load of the suburban neighborhood—the neighborhood with the highest export volumes in summer.

As the suburban neighborhood is the largest one, its influence on the ratio of exported to generated power (ϕ_E) and generated to imported power (ϕ_I) is significant. The central buy and sell prices are structured to ensure balanced benefit distribution between electricity sellers and buyers within the MNES, as explained in Eq. (3) and Eq. (4). However, grid-related costs including fees must be allocated according to actual MNES operation and are fully allocated to buyers. When the suburban neighborhood exports while the overall MNES has excess generation, both buy and sell prices decline (e.g., midday on June 3 and 6). This allocation mechanism favors importing over exporting neighborhoods. The buy price in the central optimization remains generally lower than the bi-level internal price, as costs are allocated post-optimization based on realized operation rather than anticipatory price signals. The internal price in bi-level optimization represents marginal system costs, incentivizing local generation and storage utilization. During export periods, this price converges to p_{min}, matching the central sell price at this lower bound (June 4, 5, and 7).

The fundamental difference lies in the allocation mechanism: bi-level optimization uses price signals to coordinate decentralized decisions, while central optimization distributes costs retrospectively after centralized decisions. The implemented cost allocation rule in central optimization disadvantages exporting neighborhoods, as grid costs are borne exclusively by importers regardless of which neighborhoods enabled the internal trade through their exports.

Figure 5 presents percentage cost differences between bi-level and central optimization relative to decentral optimization, disaggregated by neighborhood and season. Both bi-level and central optimization reduce total system costs by equal proportions across all seasons. Cost reduction totals 1,184 € during transition (from 7,215 € to 6,031 €), representing a 16.4 % reduction. Summer exhibits the strongest percentage reduction (65 %) as baseline costs are moderate due to high PV generation and low heating demand. Winter shows

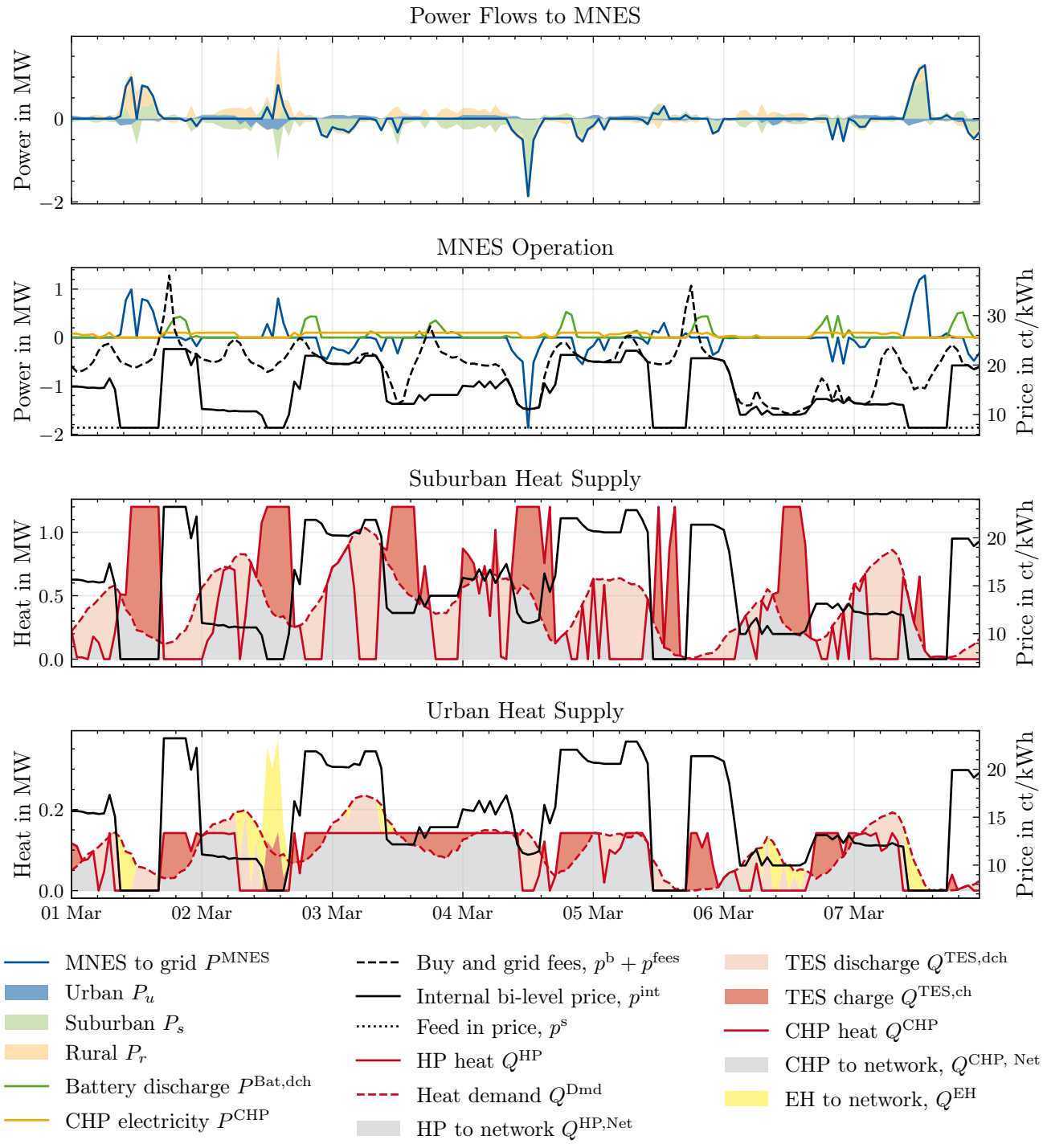

Figure 3. *Bi-level optimization results for the transition week showing power flows, internal pricing, and device operation. The first plot displays neighborhood power exchanges and resulting MNES grid flow. The second plot shows internal price dynamics, battery discharge, and CHP generation. The third and fourth plots illustrate heat pump operation in the suburban and CHP operation in the urban neighborhood. Power variables in* MW*, prices in* ct/kWh*.*

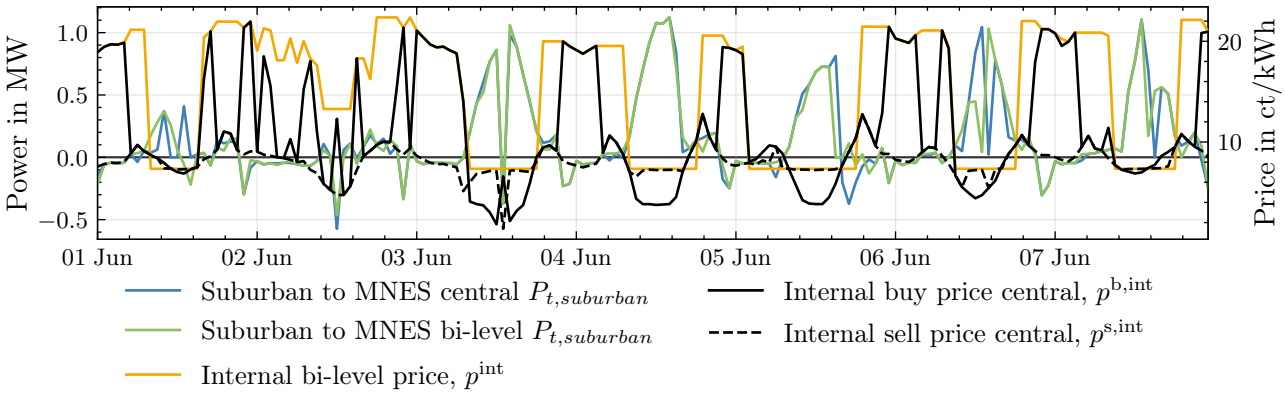

Figure 4. *Internal price comparison between central and bi-level optimization for the summer week, showing buy/sell prices in* ct/kWh *and suburban residual load in* MW*.*

substantial absolute savings (from 25,568 € to 19,450 €) despite more limited percentage reductions due to high baseline costs.

The bi-level optimization model has been demonstrated to reduce costs for all neighborhoods across all seasons. Central optimization yields heterogeneous outcomes at the neighborhood level. For instance, suburban costs increase by 41.2 % (262 €) during the summer months, despite the presence of MNES-level benefits. As previously delineated, the cost allocation rule engenders internal prices that are disadvantageous to exporting neighborhoods. Conversely, during the transition and winter seasons, central optimization has been shown to achieve cost reductions for all individual neighborhoods. Bi-level optimization prevents such disadvantages by incorporating individual neighborhood costs at the lower level, achieving comparable system-level reductions while ensuring no neighborhood faces cost increases.

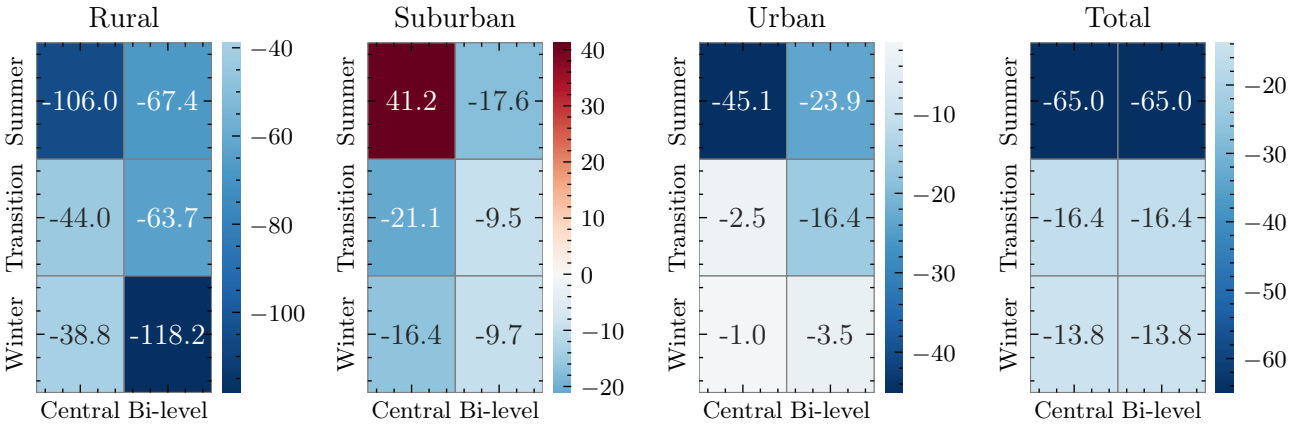

Figure 5. *Percentage cost changes relative to decentral optimization across neighborhoods, seasons, and coordination approaches. Red indicates cost increases, blue indicates reductions.*

4.3. Seasonal Effects

Generation and demand profiles, internal prices, and resulting costs vary substantially across seasons. Figure 6 displays MNES-internal energy exchange volumes across summer, transition, and winter seasons. Decentral optimization shows consistently low sharing volumes representing only coincidental alignments without coordination. Central and bi-level optimization achieve nearly identical sharing volumes across all seasons, with bi-level slightly exceeding central during transition (19.15 MWh versus 18.28 MWh).

Summer exhibits the strongest percentage cost reduction (65%) despite low absolute sharing volume (8.69 MWh bi-level, see Figure 6) due to high PV generation and low baseline costs. Negligible heating demand eliminates thermal flexibility, while battery capacity proves insufficient to store all excess renewable energy. The urban CHP remains unviable. Winter demonstrates highest absolute sharing volume (31.7 MWh bi-level) through CHP-heat pump coordination, reducing MNES import by 11 MWh and achieving 84% export avoidance. High heating demand drives elevated internal prices and near-continuous full-load operation, limiting thermal stor-

age utilization despite strong wind generation variability. The transition period achieves balanced import-export coordination (19.2 MWh bi-level) through storage-mediated temporal shifting. Partial heating requirements enable operational flexibility, while storage capacity adequately buffers predominantly solar generation. Coordination value depends on the interaction between flexibility resources, demand patterns, and external price structures. The urban neighborhood's CHP-electric heater combination provides critical counter-cyclical flexibility across all seasons by decoupling heat production from instantaneous demand through thermal storage.

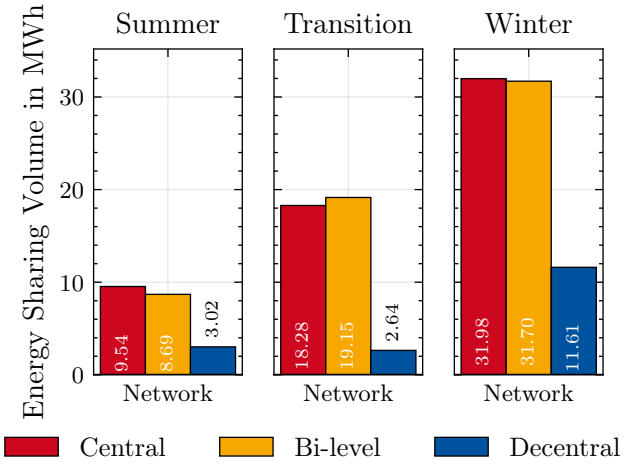

Figure 6. *Energy sharing volume across seasons and optimization approaches in* MW h. *Decentral values represent coincidental neighborhood alignments without coordination.*

5. Conclusion and Outlook

This paper presented a bi-level optimization framework for coordinating multi-neighborhood energy systems, addressing the challenge of achieving system-level efficiency while preserving neighborhood autonomy and ensuring equitable cost distribution. Using a Stackelberg game formulation reformulated as a single-level MILP, we evaluated three archetypical German neighborhoods against decentralized and centralized benchmarks for different seasons.

The bi-level optimization increases internal energy sharing by factors of nearly 3 to 7 and achieves system-level cost reductions of 13.8 % to 65 %, equivalent to a centralized approach. Critically, unlike the centralized optimization which can disadvantage individual actors (e.g., a 41.2 % cost increase for suburban neighborhood in summer), the bi-level model guarantees that no neighborhood incurs higher costs than in standalone operation. This equitable outcome is achieved by incorporating individual costs at the lower level, using price signals that reflect marginal system costs rather than imposed allocations. The internal price mechanism effectively coordinates device operation across neighborhoods. Price fluctuations between the feed-in tariff and external buy price plus fees reflect system marginal costs: during scarcity, prices signal battery and CHP operational costs; during surplus, they converge to feed-in levels. The urban neighborhood's CHP-electric heater combination provides critical counter-cyclical flexibility by decoupling heat production from instantaneous demand through thermal storage, enabling electricity generation when economically beneficial for the MNES. Conversely, summer achieves the strongest percentage cost reduction (65 %) despite more moderate sharing volumes (9.4 MWh), because baseline costs are already low due to high PV generation and minimal heating demand, with coordination mainly addressing temporal PV patterns within available battery capacity. During winter, shared energy increases threefold to 31.7 MWh, yet costs fall by only 13.8 % due to high heating demand limiting thermal flexibility. The transition periods offer optimal conditions, showing balanced import-export coordination (19.2 MWh shared) via storage-mediated shifting, as thermal storage remains flexible before heating devices reach capacity limits. Overall, this shows that coordination value depends not on exchange volume alone, but on the interaction of flexibility resources, demand patterns, and external price structures.

Future work could enhance the framework's practical applicability by evaluating alternative allocation mechanisms, different regulatory frameworks (e.g., German vs. Austrian grid fee structures), and larger, more diverse network configurations. Expanding the model to include commercial participants or dynamic market integration would also unlock further coordination potential. Additionally, an iterative price-based implementation, where neighborhoods respond to published prices without revealing private information, is an avenue for future work. The scope of the work is constrained by the simplification of network constraints and the neglect of uncertainty. These issues may be addressed in future research.

Acknowledgments

We gratefully acknowledge the financial support by the Federal Ministry for Economic Affairs and Energy (BMWE), promotional reference 03EWR010B and 03EN3080C.

References

[1] A. Nawaz, M. Zhou, J. Wu, and C. Long. A comprehensive review on energy management, demand response, and coordination schemes utilization in multi-microgrids network. In: *Applied Energy* 323 (Oct. 2022), p. 119596. ISSN: 0306-2619. DOI: 10.1016/j.apenergy.2022.119596.

[2] A. Moser. *Elektrizitätsversorgungssysteme Skriptum zur Vorlesung*. 2020th ed. Aachen: Institut für Elektrische Anlagen und Netze, Digitalisierung & Energiewirtschaft der RWTH Aachen, Aug. 2020.

[3] European University Institute. *The EU clean energy package: (2020 ed.)* LU: Publications Office, 2020. DOI: 10.2870/58299.

[4] Bundesministerium für Wirtschaft und Energie. *Entwurf eines Gesetzes zur Änderung des Energiewirtschaftsrechts zur Stärkung des Verbraucherschutzes im Energiebereich sowie zur Änderung weiterer energierechtlicher Vorschriften*. Referentenentwurf. Veröffentlicht am 11. Juli 2025. 2025.

[5] D. Ritter, P. D. D. Bauknecht, D. D. Fietze, K. Klug, and D. M. Kahles. *Energy Sharing Bestandsaufnahme und Strukturierung der deutschen Debatte unter Berücksichtigung des EU-Rechts*. Tech. rep. 46/2023. Umweltbundesamt, 2023.

[6] M. Pilz and L. Al-Fagih. *Recent Advances in Local Energy Trading in the Smart Grid Based on Game–Theoretic Approaches*. Sept. 2017. arXiv: 1702.02915 [cs].

[7] C. Marnay, S. Chatzivasileiadis, C. Abbey, R. Iravani, G. Joos, P. Lombardi, P. Mancarella, and J. Von Appen. Microgrid Evolution Roadmap. In: *2015 International Symposium on Smart Electric Distribution Systems and Technologies (EDST)*. Vienna, Austria: IEEE, Sept. 2015, pp. 139–144. ISBN: 978-1-4799-7736-9. DOI: 10.1109/SEDST.2015.7315197.

[8] P. Mancarella. MES (multi-energy systems): An overview of concepts and evaluation models. In: *Energy* 65 (Feb. 2014), pp. 1–17. ISSN: 03605442. DOI: 10.1016/j.energy.2013.10.041.

[9] Q. Wang, Z. Hou, Y. Guo, L. Huang, Y. Fang, W. Sun, and Y. Ge. Enhancing Energy Transition through Sector Coupling: A Review of Technologies and Models. In: *Energies* 16.13 (Jan. 2023), p. 5226. ISSN: 1996-1073. DOI: 10.3390/en16135226.

[10] D. Saha, N. Bazmohammadi, J. C. Vasquez, and J. M. Guerrero. Multiple Microgrids: A Review of Architectures and Operation and Control Strategies. In: *Energies* 16.2 (Jan. 2023), p. 600. ISSN: 1996-1073. DOI: 10.3390/en16020600.

[11] B. Zhou, J. Zou, C. Yung Chung, H. Wang, N. Liu, N. Voropai, and D. Xu. Multi-microgrid Energy Management Systems: Architecture, Communication, and Scheduling Strategies. In: *Journal of Modern Power Systems and Clean Energy* 9.3 (2021), pp. 463–476. ISSN: 2196-5625. DOI: 10.35833/MPCE.2019.000237.

[12] T. Sousa, T. Soares, P. Pinson, F. Moret, T. Baroche, and E. Sorin. *Peer-to-peer and community-based markets: A comprehensive review*. Dec. 2018. arXiv: 1810.09859.

[13] N. Yarar, Y. Yoldas, S. Bahceci, A. Onen, and J. Jung. A Comprehensive Review Based on the Game Theory with Energy Management and Trading. In: *Energies* 17.15 (July 2024), p. 3749. ISSN: 1996-1073. DOI: 10.3390/en17153749.

[14] W. Saad, Z. Han, H. Poor, and T. Basar. Game-Theoretic Methods for the Smart Grid: An Overview of Microgrid Systems, Demand-Side Management, and Smart Grid Communications. In: *IEEE Signal Processing Magazine* 29.5 (Sept. 2012), pp. 86–105. ISSN: 1053-5888. DOI: 10.1109/msp.2012.2186410.

[15] A. Sinha, P. Malo, and K. Deb. A Review on Bilevel Optimization: From Classical to Evolutionary Approaches and Applications. In: *IEEE Transactions on Evolutionary Computation* 22.2 (Apr. 2018), pp. 276–295. ISSN: 1089-778X, 1089-778X, 1941-0026. DOI: 10.1109/tevc.2017.2712906.

[16] B. Zhang, Q. Li, L. Wang, and W. Feng. Robust optimization for energy transactions in multi-microgrids under uncertainty. In: *Applied Energy* 217 (May 2018), pp. 346–360. ISSN: 03062619. DOI: 10.1016/j.apenergy.2018.02.121.

[17] S. E. Ahmadi, D. Sadeghi, M. Marzband, A. Abusorrah, and K. Sedraoui. Decentralized bi-level stochastic optimization approach for multi-agent multi-energy networked micro-grids with multi-energy storage technologies. In: *Energy* 245 (Apr. 2022), p. 123223. ISSN: 03605442. DOI: 10.1016/j.energy.2022.123223.

[18] G. Zhang, G. Zhang, Y. Gao, and J. Lu. Competitive Strategic Bidding Optimization in Electricity Markets Using Bilevel Programming and Swarm Technique. In: *IEEE Transactions on Industrial Electronics* 58.6 (June 2011). doi:10.1109/TIE.2010.2055770, pp. 2138–2146. ISSN: 0278-0046, 1557-9948.

[19] Q. Hong and F. Meng. Customized Multi-energy Pricing in Smart Grids: A Bilevel and Evolutionary Computation Approach. In: *Advances in Computational Intelligence Systems*. Ed. by G. Panoutsos, M. Mahfouf, and L. S. Mihaylova. Vol. 1454. Cham: Springer Nature Switzerland, 2024, pp. 475–488. ISBN: 978-3-031-55567-1 978-3-031-55568-8. DOI: 10.1007/978-3-031-55568-8_40.

[20] J. Wang, Y. Gao, and R. Li. Reinforcement learning based bilevel real-time pricing strategy for a smart grid with distributed energy resources. In: *Applied Soft Computing* 155 (Apr. 2024), p. 111474. ISSN: 15684946. DOI: 10.1016/j.asoc.2024.111474.

[21] T. Lu, Q. Ai, and Z. Wang. Interactive game vector: A stochastic operation-based pricing mechanism for smart energy systems with coupled-microgrids. In: *Applied Energy* 212 (Feb. 2018), pp. 1462–1475. ISSN: 03062619. DOI: 10.1016/j.apenergy.2017.12.096.

[22] H. Karimi, R. Bahmani, S. Jadid, and A. Makui. Dynamic transactive energy in multi-microgrid systems considering independence performance index: A multi-objective optimization framework. In: *International Journal of Electrical Power & Energy Systems* 126 (Mar. 2021), p. 106563. ISSN: 01420615. DOI: 10.1016/j.ijepes.2020.106563.

[23] A. Jani and S. Jadid. Two-stage energy scheduling framework for multi-microgrid system in market environment. In: *Applied Energy* 336 (Apr. 2023), p. 120683. ISSN: 03062619. DOI: 10.1016/j.apenergy.2023.120683.

[24] Y. Zhuang, L. Cheng, N. Qi, H. Li, Z. Li, and C. Wang. Optimal Energy Management for Multi-Microgrid System Based on Stackelberg Game. In: *2023 IEEE PES Innovative Smart Grid Technologies Europe (ISGT EUROPE)*. Grenoble, France: IEEE, Oct. 2023, pp. 1–5. ISBN: 979-8-3503-9678-2. DOI: 10.1109/ISGTEUROPE56780.2023.10408485.

[25] M. H. S. Boloukat and A. A. Foroud. Multiperiod Planning of Distribution Networks Under Competitive Electricity Market With Penetration of Several Microgrids, Part I: Modeling and Solution Methodology. In: *IEEE Transactions on Industrial Informatics* 14.11 (Nov. 2018), pp. 4884–4894. ISSN: 1551-3203, 1941-0050. DOI: 10.1109/TII.2018.2807396.

[26] Y. Fu, Z. Zhang, Z. Li, and Y. Mi. Energy Management for Hybrid AC/DC Distribution System With Microgrid Clusters Using Non-Cooperative Game Theory and Robust Optimization. In: *IEEE Transactions on Smart Grid* 11.2 (Mar. 2020), pp. 1510–1525. ISSN: 1949-3053, 1949-3061. DOI: 10.1109/TSG.2019.2939586.

[27] Y. Matamala, T. K. Das, and F. Feijoo. A stochastic Stackelberg problem with long-term investment decisions in Power-To-X technologies for multi-energy microgrids. In: *Energy* 314 (Jan. 2025), p. 134131. ISSN: 03605442. DOI: 10.1016/j.energy.2024.134131.

[28] Y. Lin, P. Dong, X. Sun, and M. Liu. Two-level game algorithm for multi-microgrid in electricity market. In: *IET Renewable Power Generation* 11.14 (Dec. 2017), pp. 1733–1740. ISSN: 1752-1416, 1752-1424. DOI: 10.1049/iet-rpg.2017.0212.

[29] M. Schmidt and Y. Beck. *A Gentle and Incomplete Introduction to Bilevel Optimization*. Trier, June 2021.

[30] M. Hoffmann, L. Kotzur, and D. Stolten. The Pareto-optimal temporal aggregation of energy system models. In: *Applied Energy* 315 (June 2022), p. 119029. ISSN: 0306-2619. DOI: 10.1016/j.apenergy.2022.119029.

[31] Deutscher Wetterdienst. *Wetter und Klima - Deutscher Wetterdienst - Wetter- und Klimalexikon*. 10.10.25.

[32] Bundesnetzagentur. *SMARD – Marktdatenvisualisierung der Bundesnetzagentur*. 13.11.25.

[33] J. Krassowski and J. Benthin. *Integrierte Betrachtung von Strom-, Gas- und Wärmesystemen zur modellbasierten Optimierung des Energieausgleichs- und Transportbedarfs innerhalb der deutschen Energienetze*. Tech. rep. Oberhausen/Essen: Fraunhofer UMSICHT und GWI Essen, Mar. 2020.

[34] S. Henn, J. D. Schölzel, T. Beckhölter, C. Wüller, R. Hamze, and D. Müller. Districtgenerator: Generating building-specific load profiles for residential districts. In: *Journal of Open Source Software* 10.111 (2025), p. 7657. DOI: 10.21105/joss.07657.

[35] M. Wirtz, P. Remmen, and D. Müller. EHDO: A free and open-source webtool for designing and optimizing multi-energy systems based on MILP. In: *Computer Applications in Engineering Education* 29.5 (2021), pp. 983–993. ISSN: 1099-0542. DOI: 10.1002/cae.22352.

[36] Deutsche Energie-Agentur GmbH (dena). *Begleitdokument KWW-Technikkatalog Wärmeplanung*. Tech. rep. Technology catalog for municipal heat planning. Berlin, Germany: Deutsche Energie-Agentur GmbH, 2025.